New Phytologist

Research

The carnivorous Venus flytrap uses prey-derived amino acid carbon to fuel respiration

Lukas Fasbender[1], Daniel Maurer[2], Jürgen Kreuzwieser[2], Ines Kreuzer[3], Waltraud X. Schulze[4], Jörg Kruse[2], Dirk Becker[3], Saleh Alfarraj[5], Rainer Hedrich[3,5], Christiane Werner[1] and Heinz Rennenberg[2,5]

[1]Institute of Forest Sciences, Chair of Ecosystem Physiology, University of Freiburg, Georges-Köhler-Allee 53/54, Freiburg 79110, Germany; [2]Institute of Forest Sciences, Chair of Tree Physiology, University of Freiburg, Georges-Köhler-Allee 53/54, Freiburg 79110, Germany; [3]Institute for Molecular Plant Physiology and Biophysics, University of Würzburg, Würzburg 97070, Germany; [4]Department of Plant Systems Biology, University of Hohenheim, Stuttgart 70593, Germany; [5]College of Science, King Saud University, PO Box 2455, Riyadh 11451, Saudi Arabia

Author for correspondence:
Heinz Rennenberg
Tel: +49 761 2038300
Email: heinz.rennenberg@ctp.uni-freiburg.de

Received: *12 October 2016*
Accepted: *23 November 2016*

New Phytologist (2017) **214:** 597–606
doi: 10.1111/nph.14404

Key words: amino acid catabolism, carbon partitioning, *Dionaea muscipula* (Venus flytrap), glutamine, nitrogen (N) partitioning, plant carnivory, respiratory degradation.

Summary

- The present study was performed to elucidate the fate of carbon (C) and nitrogen (N) derived from protein of prey caught by carnivorous *Dionaea muscipula*. For this, traps were fed $^{13}C/^{15}N$-glutamine (Gln).
- The release of $^{13}CO_2$ was continuously monitored by isotope ratio infrared spectrometry. After 46 h, the allocation of C and N label into different organs was determined and tissues were subjected to metabolome, proteome and transcriptome analyses.
- Nitrogen of Gln fed was already separated from its C skeleton in the decomposing fluid secreted by the traps. Most of the Gln-C and Gln-N recovered inside plants were localized in fed traps. Among nonfed organs, traps were a stronger sink for Gln-C compared to Gln-N, and roots were a stronger sink for Gln-N compared to Gln-C. A significant amount of the Gln-C was respired as indicated by ^{13}C-CO_2 emission, enhanced levels of metabolites of respiratory Gln degradation and increased abundance of proteins of respiratory processes. Transcription analyses revealed constitutive expression of enzymes involved in Gln metabolism in traps.
- It appears that prey not only provides building blocks of cellular constituents of carnivorous *Dionaea muscipula*, but also is used for energy generation by respiratory amino acid degradation.

Introduction

In its natural environment in North and South Carolina, the Venus flytrap (*Dionaea muscipula*) has only limited access to nutrients required for growth and development from soil-derived sources (Roberts & Oosting, 1958; Brewer *et al.*, 2011). Considerable amounts of minerals may only become available in the soil during sporadic fire events (Roberts & Oosting, 1958). To overcome this constraint and to compete successfully with other vegetation components, *D. muscipula* attracts insects by shape and color of traps (Joel *et al.*, 1985; Ichiisi *et al.*, 1999; Schaefer & Ruxton, 2008; Kurup *et al.*, 2013) and by the emission of volatile organic compounds that simulate the smell of food (Kreuzwieser *et al.*, 2014). *Dionaea* captures attracted insects with active snap traps closing in fractions of a second after repetitive mechano-stimulation of trigger hairs by the victim (Escalante-Pérez *et al.*, 2011; Böhm *et al.*, 2016a). It digests its prey in the hermetically closed traps by the release of an acidic enzyme cocktail mediating de-polymerization of macro-molecules by hydrolysis (Schulze *et al.*, 2012; Libiakova *et al.*, 2014; Paszota *et al.*, 2014; Böhm *et al.*, 2016a,b); it retrieves prey-derived organic compounds and ions by activation of transport processes (Scherzer *et al.*, 2013, 2015; Kruse *et al.*, 2014; Böhm *et al.*, 2016a,b).

For growth and development of *Dionaea*, acquisition of nitrogen (N) from prey is of particular significance (Brewer *et al.*, 2011; Kruse *et al.*, 2014; Gao *et al.*, 2015). N is present in prey mainly in the form of chitin and protein (Mariod *et al.*, 2011; Finke, 2013). Hydrolysis of these macro-molecules to the monomeric constituents by chitinase and peptidase takes place in the closed traps that act as a 'green stomach'. The prey-decomposing fluid containing these hydrolytic enzymes is provided by the gland-based secretory system on the inner surface of the traps (Schulze *et al.*, 2012; Libiakova *et al.*, 2014; Paszota *et al.*, 2014; Bemm *et al.*, 2016). Amino acids produced by peptidase activity in the prey-decomposing fluid are thought to be taken up into trap tissue. However, in recent trap feeding experiments with $^{13}C/^{15}N$-labeled glutamine (Gln) or $^{13}C/^{15}N$-labeled insect powder, ^{15}N-label was recovered in fed traps and preferentially distributed to newly developing traps, but ^{13}C-label could not be retrieved (Kruse *et al.*, 2014; Gao *et al.*, 2015). In addition, feeding of traps with unlabeled Gln inhibited ^{15}N influx from root-absorbed $^{13}C/^{15}N$-Gln into the traps, whereas influx

of ^{13}C into the traps from labeled Gln was maintained. Apparently, fed traps constitute a carbon (C) sink that even uses organic C from the roots. A high demand for organic C will develop in traps upon prey capture from the requirement to generate energy for trap closure and prey retention, as well as sustained production and release of the prey-decomposing cocktail from the glands at low photosynthetic activity (Pavlovic *et al.*, 2010, 2011; Kruse *et al.*, 2014). This is indicated by a loss of ATP (Jaffe, 1973; Williams & Bennett, 1980) and an increased rate of respiration (Pavlovic *et al.*, 2010, 2011; Kruse *et al.*, 2014). Based on these findings it is hypothesized that (1) N from prey-derived amino acids may be separated inside trap tissue from its C backbone, and may be subjected to long-distance transport in phloem and xylem to developing tissues; and (2) the C backbone of amino acids may be channeled into the TCA cycle for energy production by respiration and may be released as CO_2 into the atmosphere (Kruse *et al.*, 2014; Gao *et al.*, 2015).

To trace the destiny of prey-derived N and C in *Dionaea* plants, we here fed flytraps with highly enriched $^{13}C/^{15}N$-Gln and monitored the release of $^{13}CO_2$ continuously online. The distribution of ^{13}C- and ^{15}N-label in fed traps and unfed plant organs of the carnivorous plant was analyzed after 46 h of exposure at ongoing consumption of the Gln fed. In addition, we determined the consequences of trap feeding for primary metabolite abundance as well as protein levels and gene expression of enzymes known to be involved in respiratory glutamate (Glu) catabolism (Hildebrandt *et al.*, 2015). Our results show that carnivorous *D. muscipula* can use prey-derived amino acids as both a source of N for growth and development of the entire plant, and as an alternative respiratory substrate to fuel the energy demand for prey digestion.

Materials and Methods

Plant material and feeding experiments

Dionaea muscipula Ellis plants were purchased from a commercial supplier and grown for 3–4 months in a glasshouse at 24 ± 4°C supplied with slow-release fertilizer and rainwater. Under these conditions, plants had limited access to mineral nutrients, resulting in a low N status (Kruse *et al.*, 2014). For feeding experiments plants were transferred into 250 cm^3 plastic pots containing nutrient-poor peat as substrate and grown in climate-controlled cabinets (HPS 1500; Heraeus Vötsch, Hanau, Germany) at day : night cycles of 16 h : 8 h, 25 : 20°C and 150 µmol m^{-2} s^{-1} photosynthetically active radiation during the light period. Plants were allowed to acclimatize to these growth conditions for 12 d receiving deionized water daily.

Feeding was performed with uniform ^{13}C and ^{15}N double labeled L-Gln (99% labeled each, Cambridge Isotope Laboratories, Inc., Tewksbury, MA, USA) by applying 1 mg $^{13}C/^{15}N$-Gln mixed into 25 µl deionized water on three traps per plant. To prevent any loss of label and to facilitate the digestion process, the solution was pipetted onto a punched-out round piece of cellulose filter (Schleicher & Schuell GmbH, Dassel, Germany), 6 mm in diameter, that was covered with 10 mg homogenized and dried insect paste and applied to each trap (Kruse *et al.*, 2014). Trap closure and digestion were triggered by mechanically stimulating the hairs inside the *Dionaea* traps (Böhm *et al.*, 2016a,b). Immediately after labeling, the plants were placed into 1 liter (110 mm diameter, 200 mm height) borosilicate enclosures (Zitt-Thoma GmbH, Freiburg, Germany). Four enclosures were interfaced to a Delta Ray Isotope Ratio Infrared Spectrometer (Thermo Fisher Scientific, Bremen, Germany) for continuous measurement of $^{12}CO_2$: $^{13}CO_2$ and CO_2 concentrations, respectively. Air temperature and relative air humidity were recorded downstream to each enclosure by Voltcraft DL-120 TH data loggers (Conrad Electronic SE, Hirschau, Germany). The enclosures were placed into climate-controlled cabinets set up with the plant's growth conditions (see 'Feeding experiments' above). They were permanently flushed with synthetic air (Messer Industriegase GmbH, Bad Soden, Germany) containing 405.6 ± 0.2 p.p.m. CO_2 at a rate of 200 ml min^{-1} to maintain steady state conditions. Gas samples from three plant-containing enclosures and one empty control enclosure were connected to a valve system which selected the samples to be continuously analyzed by isotope laser spectroscopy. The measuring interval for each chamber was 9 min h^{-1}.

After 46 h of each experiment, when traps were still in the process of consuming the Gln fed, Gln-fed plants were completely harvested and separated into Gln-fed and nonfed traps, leaves attached to fed and nonfed traps, fine roots and coarse roots. A total of six nonfed control plants were harvested in the same manner. Plant tissues were immediately shock-frozen in liquid N and stored at −80°C. Aliquots of the tissues were oven-dried and analyzed for stable C and N isotope abundance as well as total C and N contents.

Quantification of $^{13}CO_2$ emission from $^{13}C/^{15}N$-Gln

Quantification of ^{13}C emissions (nmol min^{-1} g^{-1} DW) was based (1) on the differences in CO_2 concentrations between the outlets of the empty control enclosure and the plant-containing enclosures as continuously analyzed by the Delta Ray Isotope Ratio Infrared Spectrometer (Thermo Fisher Scientific). We considered (2) the $\delta^{13}C$ values at enclosure outlets to calculate the total flux of $^{13}CO_2$ from the plants. The incoming air contained 405.6 ± 0.2 p.p.m. CO_2 with a $\delta^{13}CO_2$ value of -5.63 ± 0.11‰ at the given flow rate of 200 ml min^{-1}. To account for the isotopic effect of photosynthetic discrimination in the light and the $^{13}CO_2$ evolved from respiratory ^{13}C-Gln degradation, we calculated the net $^{13}CO_2$ flux in the chambers. Before the onset of Gln degradation, differences between the control enclosures and the plant-containing enclosures revealed an average net $^{13}CO_2$ uptake per plant of -8.7 ± 0.9 nmol min^{-1} ($n = 9$). All $^{13}CO_2$ flux rates higher than these initial values measured from ($^{13}C/^{15}N$)-Gln fed plants were assumed to originate from the Gln-tracer. This is a conservative approach to estimate the $^{13}CO_2$ released from respiration of fed Gln, since photosynthetic re-fixation of respired $^{13}CO_2$ is not considered; therefore, the $^{13}CO_2$ emission rates given constitute minimum values of respired ^{13}C-tracer.

Total C and N content; $\delta^{13}C$- and $\delta^{15}N$-enrichment

Aliquots of 1–2 mg oven dried, pulverized plant tissue were weighed into tin capsules for total C and total N as well as stable C and N isotope analyses. Samples were combusted in an element analyzer (NA 2500; CE Instruments, Milan, Italy) coupled to an isotope ratio mass spectrometer (Delta Plus; Finnigan MAT, Bremen, Germany) via a Conflow II interface (Thermo-Finnigan MAT). To determine instrument drift and isotope linearity of the system, Glu with known isotope ratios was included as laboratory standard at different weights in every sequence of samples. Relative abundances (R) of stable isotopes in plant tissue, that is $^{13}C:{}^{12}C$ and $^{15}N:{}^{14}N$ ratios, were calculated as relative deviation from international standards (for ^{13}C, Vienna Pee Dee belemnite; for ^{15}N, atmospheric N_2) applying the δ annotation (Eqn 1):

$$\delta_{sample} = \left[\left(R_{sample}/R_{standard}\right) - 1\right] \times 1000 \qquad \text{Eqn 1}$$

Instrument precision amounted to $0.3 \pm 0.2‰$ for both $\delta^{13}C$ and $\delta^{15}N$. Enrichment of different tissues in ^{13}C and ^{15}N above control levels was determined in response to feeding $^{13}C/^{15}N$-Gln. For enrichment of tissues in ^{15}N ($^{15}N_S$), Eqn 2 was applied:

$$^{15}N_S\left(\mu mol\, g^{-1}\right) = \left[\left(N_S \times atom\%^{15}N_S \times 10^{-2}\right) - \left(N_C \times atom\%^{15}N_C \times 10^{-2}\right)\right] 15^{-1} \qquad \text{Eqn 2}$$

where $^{15}N_S$ is the enrichment of tissues (fed traps, nonfed traps, petioles of fed traps and nonfed traps, roots), N_S the N concentration of enriched tissues ($\mu g\, g^{-1}$ DW), atom% $^{15}N_S$ the ^{15}N abundance of enriched tissues, and N_C and atom% $^{15}N_C$ the respective values of control tissues ($n = 9$) indicating the natural isotope abundances. By taking the biomass of each tissue into account, ^{15}N enrichment per tissue and recovery of the ^{15}N applied in each tissue were calculated. A similar calculation for ^{13}C enrichment above control levels was performed neglecting variation of ^{13}C natural abundance by gas exchange (Farquhar *et al.*, 1989).

Metabolome analyses

Relative abundances of polar low-molecular-weight metabolites present in above-ground *Dionaea* tissues were analyzed by GC-MS. For this, metabolites were extracted and derivatized using a modification of the method described by Kreuzwieser *et al.* (2009). Harvested plant material was quickly snap frozen in liquid N_2 and stored at −80°C until analysis. Approximately 30 mg of frozen sample material was weighed into a cooled 1.5 ml reaction tube containing 500 µl cold 85% methanol and 100 ng μl^{-1} ribitol as internal standard. Tubes were vortexed briefly, heated to 65°C and shaken at 1400 r.p.m. for 15 min. Samples were then centrifuged at 14 000 *g* for 10 min; an aliquot of 80 µl of the supernatant was freeze-dried overnight. For derivatization, 10 µl of a 20 mg ml^{-1} solution of methoxyamine hydrochloride in anhydrous pyridine (Sigma-Aldrich Inc., Steinheim, Germany) was added to the dried extracts and samples were incubated at 30°C for 90 min with shaking at 1400 r.p.m. Thereafter, 15 µl *N*-methyl-N-(trimethylsilyl)-trifluoroacetamide (MSTFA; Sigma-Aldrich) was added and samples were incubated at 37°C for 30 min with shaking at 1400 r.p.m. Before GC-MS analysis, 5 µl of an n-alkane retention index calibration mixture was added and samples were transferred to GC-MS vials. Samples were then analysed on a GC-MS system (Agilent GC 6890N coupled to a 5975C quadrupole MS detector; Agilent Technologies, Palo Alto, CA, USA) equipped with an autosampler (MultiPurpose Sampler MPS2; Gerstel, Mülheim, Germany). All devices were controlled by the Agilent MASSHUNTER software (Agilent Technologies). Aliquots of 1 µl derivatized sample were injected in splitless mode into the system, and separated on a capillary column (HP-5 ms ultra inert, 0.25 mm ID, 0.25 µm film thickness, 30 m length; Agilent Technologies). Run conditions as well as MS settings were as described by Kreuzwieser *et al.* (2009). Analysis of raw data including peak detection, peak alignment and identification of compounds based on matching with the Golm Metabolome Database (Kopka *et al.*, 2005) was performed with the Quantitative Analysis Module of the MASSHUNTER software (Agilent Technologies). Moreover, authentic standards were used for peak identification. Peak areas were normalized using the peak area of the internal standard, ribitol, and the fresh weight of samples. Artefact peaks and common contaminants were identified by analysis of 'blank' samples prepared in the same manner as biological samples. Signals corresponding to these artefacts were omitted from biological interpretation.

Gene expression analyses

RNA was isolated separately from each sample of fed traps, nonfed traps, leaves of fed traps and leaves of nonfed traps using a modified cetyltrimethylammonium bromide (CTAB)-based protocol. In brief, 0.1 g plant material powdered in liquid N was thoroughly mixed with 0.7 ml of hot (65°C) RNA extraction buffer (2% CTAB, 2% polyvinylpyrrolidone K 25 (PVP), 100 mM Tris/HCl, pH 8.0, 25 mM Na-EDTA, pH 8.0, and 2 M NaCl; 2.5% (v/v) 2-mercaptoethanol was added immediately before use). Following 10 min of incubation at 65°C and extraction with 1 volume of chloroform : isoamyl alcohol (24 : 1, v/v), RNA was precipitated from the supernatant by adding 175 µl of 8 M LiCl overnight (4°C). RNA was collected by centrifugation, resuspended in diethylpyrocarbonate (DEPC)-treated H_2O and precipitated in the presence of 0.1 volume of 3 M Na-acetate (pH 5.2) and 2.5 volumes of 96% EtOH. After a washing step using 70% EtOH, RNA was finally dissolved in 40 µl of DEPC-H_2O. DNA contamination was removed by DNase I treatment on a column (Roche, Basel, Switzerland). RNA quantity and quality were determined by capillary electrophoresis (Experion Automated Electrophoresis System and Experion RNA HighSense Analysis Kit; Bio-Rad Laboratories, Hercules, CA, USA).

Individual transcript levels were analyzed by quantitative real-time PCR (qRT-PCR). qRT-PCR was performed using a Realplex Mastercycler (Eppendorf, Hamburg, Germany), 1 : 20

diluted cDNA and the ABsolute QPCR SYBR Green Capillary Mix (Thermo Scientific, Waltham, MA, USA). Expression levels were quantified using a standard for each primer pair and normalized to 10 000 molecules of actin (DmACT) cDNA transcripts. Gene-specific primers were designed using the software LightCycler Probe Design 2.0 (Roche Life Science, Penzberg, Germany) based on the transcriptomic information available under http://tbro.carnivorom.com (release 1.03; Bemm *et al.*, 2016). Individual transcripts deposited there are given in parentheses. The following primers were used: actin (comp226979_c1_seq1), primer pair DmACTfw 5′-TCTTTGATTG GGATGGAAGC-3′ and DmACTrev 5′-GCAATGCCAG GGAACATAGT-3; asparagine synthetase (comp216588_c0_seq2), primer pair DmASN1fw 5′-TGGTCTAAGAATCTGGA-3′ and DmASN1rev 5′-AGTTTACACGCAATGAA-3′; Glu decarboxylase (comp234222_c2_seq2), primer pair, DmGADfw 5′-TCTGAAGAAGGAAAGGC-3′ and DmGADrev 5′-ACTA TGCGTTTACAGAA-3′; 4 aminobutyrate-pyruvate transaminase (comp216013_c0.0_seq2), primer pair DmPOP2fw 5′-TAAGTCACCTACTGATCC-3′ and DmPOP2rev 5′-GG GTAATGAATCCAGC; Glu dehydrogenase (comp228208_c1.1_seq4), primer pair DmGDH2fw 5′-GAGCGTTTCTGAA CAT-3′ and DmGDH2rev 5′-CAAATCACCTTTAGTTGC-3′; oxoglutarate dehydrogenase (comp133088_c0_seq1), primer pair DmOGDHCfw 5′-GCCGAGGTAATATAGATG-3′ and DmOGDHCrev 5′- ATGACTCCAGGAATTTAG-3′.

Proteomic analyses

Powdered plant material was extracted in 6 M urea, 2 M thiourea and 10 mM Tris/HCl, pH 8. A total of 10 µg protein was then digested with trypsin as previously described (Wu & Schulze, 2015). Tryptic peptide mixtures were analyzed by LC/MS/MS using a nanoflow Easy-nLC1000 (Thermo Scientific) as an HPLC system and a Quadrupole-Orbitrap hybrid mass spectrometer (Q-Exactive Plus, Thermo Scientific) as mass analyzer. Peptides were eluted from a 75 µm × 50 cm analytical column (Thermo Scientific) on a linear gradient running from 4 to 64% acetonitrile in 240 min and sprayed directly into the LTQ-Orbitrap mass spectrometer. Proteins were identified by MS/MS using information-dependent acquisition of fragmentation spectra of multiple charged peptides. Up to 12 data-dependent MS/MS spectra were acquired for each full-scan spectrum obtained at 60 000 full-width half-maximum resolution. Overall cycle time was *c.* 1 s.

Protein identification and ion intensity quantification were carried out by MaxQuant, v.1.4.1.2 (Cox & Mann, 2008). Spectra were matched against the assembled transcriptome of *D. muscipula* (Bemm *et al.*, 2016; 194 308 contigs) using Andromeda (Cox *et al.*, 2011). Thereby, carbamidomethylation of cysteine was set as a fixed modification and oxidation of methionine as variable modification. Mass tolerance for the database search was set to 20 p.p.m. on full scans and 0.5 Da for fragment ions. Multiplicity was set to 1. For label-free quantification, retention time matching between runs was chosen within a time window of 2 min. Peptide false discovery rate (FDR) and protein FDR were set to 0.01, while site FDR was set to 0.05. Hits to contaminants (e.g. keratins) and reverse hits identified by MaxQuant were excluded from further analysis.

Reported ion intensity values of extracted ion chromatograms were used for quantitative data analysis. cRacker (Zauber & Schulze, 2012) was used for label-free data analysis based on the MaxQuant output (evidence.txt). All proteotypic nonphosphopeptides were used for quantification. Within each sample, ion intensities of each peptide ion species (each *m*/*z*) were normalized against total ion intensities in the sample (peptide ion intensity/total sum of ion intensities). Subsequently, each peptide ion species (i.e. each *m*/*z* value) was scaled against the average normalized intensities of that ion across all treatments. Normalized peptide ion intensities were then summed to protein intensities.

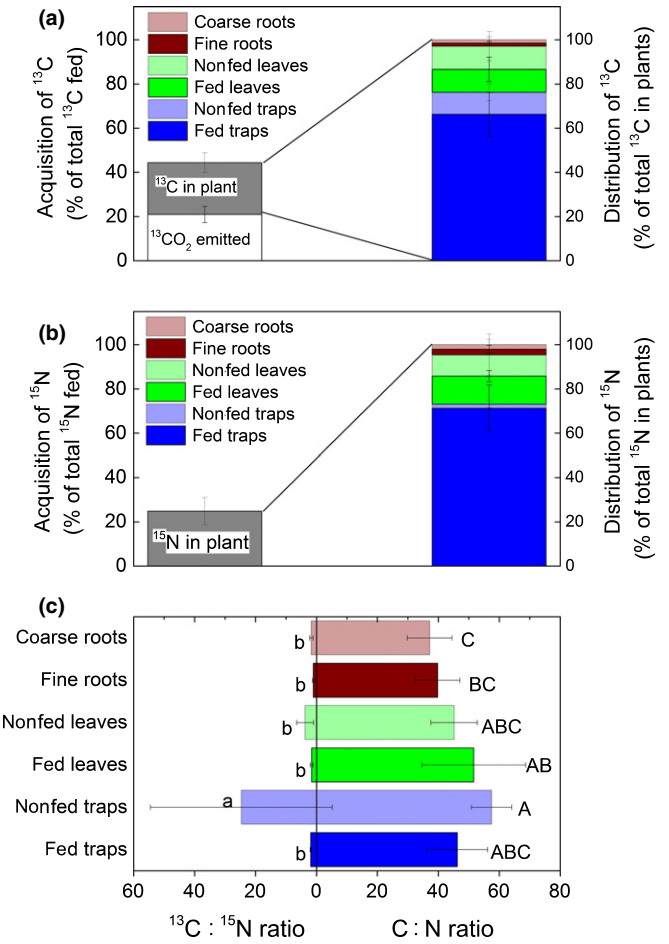

Fig. 1 Acquisition and plant internal distribution of ^{13}C and ^{15}N derived from (^{13}C/^{15}N)-Gln fed to *Dionaea* traps. (a) ^{13}C, (b) ^{15}N, (c) ^{13}C : ^{15}N and C : N ratios of *Dionaea* plants after feeding (^{13}C/^{15}N)-Gln. Three traps of each *Dionaea* plant were fed with 1 mg ^{13}C/^{15}N-labeled Gln per trap for 46 h. The plants ($n = 9$) were harvested and separated into the tissues indicated. ^{13}C and ^{15}N contents were determined by IRMS. Quantification of ^{13}C and ^{15}N taken up and distributed within the plants was based on total dry mass of the individual tissues and the ^{13}C and ^{15}N contents. Data shown are means ± SD of nine independent experiments. Statistically significant differences between C : N ratios in (c) were calculated by ANOVA followed by a Tukey post-hoc test at $P \leq 0.05$ and are shown by different letters beside bars.

Values from three biological replicates were averaged after normalization and scaling.

Statistical analyses

Normal distribution of the data was tested using the Shapiro–Wilk test, and the homogeneity of variances was tested operating the Levene[2] test (both $P = 0.05$). One-way ANOVA ($P = 0.05$, $\alpha = 0.95$, Fisher's *post-hoc* test) was used to determine significant differences between the treatments. The software ORIGIN PRO 9.1 (OriginLab Corp., Northampton, MA, USA) was used for the statistical analyses.

Results

When traps of *Dionaea* were fed $^{13}C/^{15}N$-Gln, we found that 45% of the ^{13}C-label, but only 25% of the ^{15}N-label was retrieved by the traps within 46 h (Fig. 1). Apparently N of prey-derived amino compounds already becomes separated from its C skeleton by the prey-decomposing fluid secreted by gland cells into the external stomach. With 46 h of exposure, about half of ^{13}C-label taken up was respired and emitted as $^{13}CO_2$ into the atmosphere (Figs 1a, 2). Respiration of Gln-derived C initially increased with time of exposure (Fig. 2), as indicated by a pronounced increase in respiratory $^{13}CO_2$ release. After *c.* 25 h, emission of Gln-derived $^{13}CO_2$ reached a maximum and declined during subsequent exposure (Fig. 2). The flux of $^{13}CO_2$ was significantly higher in the dark than in the light, indicating partial inhibition of the TCA cycle (Tcherkez *et al.*, 2008; Priault *et al.*, 2009) in the light.

The majority of Gln-derived ^{13}C recovered inside the plants was found in fed traps (66% of total Gln-derived C); most of the remaining Gln-derived ^{13}C recovered inside plants was about equally distributed between the leaves of fed traps, non-fed traps and their leaves. It amounted to *c.* 10% of total ^{13}C inside plants for each of these organs. Only a minor portion of the ^{13}C-label recovered was allocated to the roots (< 3%) (Fig. 1a).

Similar to ^{13}C, the ^{15}N from the Gln fed to the traps was also recovered inside the plant mainly in the fed traps (71%) (Fig. 1b). However, the distribution of ^{15}N to other organs differed considerably from ^{13}C distribution. Leaves of fed traps contained 13% and leaves of nonfed traps 10% of the ^{15}N label, whereas nonfed traps contained <2% (Fig. 1b). Nonfed traps appear to be a much stronger sink for prey-derived ^{13}C compared to ^{15}N. This difference between ^{13}C and ^{15}N acquisition of nonfed traps is also indicated by a strongly enhanced $^{13}C:{}^{15}N$ ratio compared to all other tissues analyzed (Fig. 1c). The generally high but similar C : N ratios of *Dionaea* organs (Fig. 1c) are due to the relatively low N contents of *Dionaea* tissues (Kruse *et al.*, 2014). With *c.* 5% of the ^{15}N recovered, the roots were a stronger sink for ^{15}N than for ^{13}C (Fig. 1a,b).

Consistent with the emission of $^{13}CO_2$ derived from trap-fed Gln, the levels of metabolites of respiratory Gln degradation increased, particularly Gln itself and metabolites involved in the TCA cycle (Supporting Information Table S1; Figs 3, S1). Consistent with the assumption that the C-skeleton of Gln is used for respiratory energy gain, the levels of 2-oxoglutarate increased significantly. Slightly increased levels were also detected for fumarate and malate, but not for succinate, citrate or Glu. In addition, levels of amino acids of the pyruvate (alanine (Ala), valine (Val)) and aspartate (aspartic acid (Asp), isoleucine (Ile)) families were enhanced indicating the use of N derived from trap-fed Gln in different primary metabolic processes. The observation of elevated serine (Ser) levels in response to trap-fed Gln (Table S1) is consistent with prey-mediated stimulation of sulfur metabolism, since Ser is a direct precursor of cysteine (Cys) (Rennenberg & Herschbach, 2014). Stimulation of sulfur metabolism seems to be required for prey digestion in order to produce and secrete sulfur-rich hydrolytic enzymes into the 'outer stomach' of the traps for prey digestion (Rainer Hedrich, Heinz Rennenberg, unpublished results).

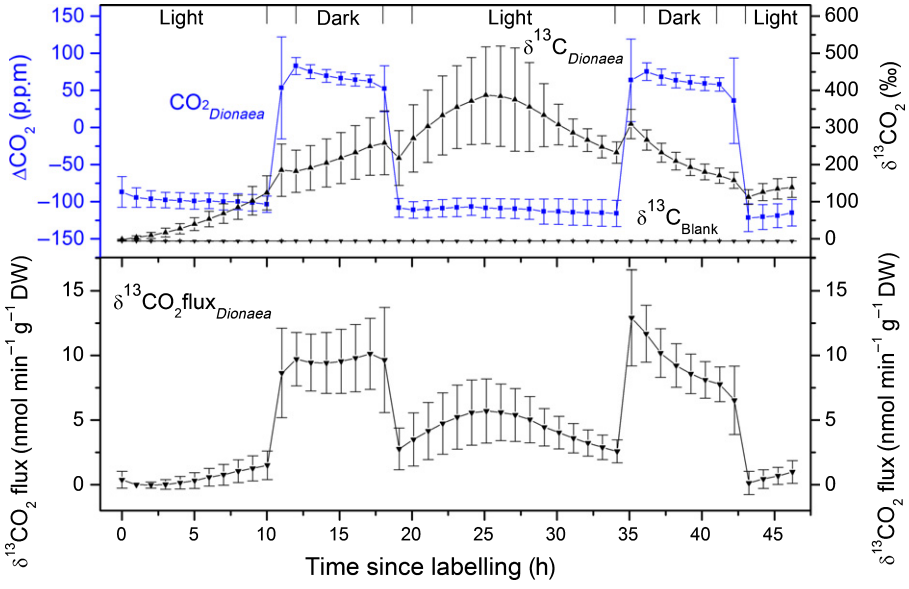

Fig. 2 CO_2 gas exchange of *Dionaea* plants fed $^{13}C/^{15}N$-Gln to the traps. Three traps of a *Dionaea* plant were fed with 1 mg $^{13}C/^{15}N$-labeled Gln each and placed into enclosures. CO_2 concentrations as well as $\delta^{13}C$ signatures were determined by laser spectrometry; net flux rates of $^{13}CO_2$ were calculated as described in the Materials and Methods section. Upper, CO_2 difference between empty enclosure and plant enclosure, and $\delta^{13}C$ signatures in the plant enclosure. Lower, net flux of $^{13}CO_2$ from *Dionaea* plants. Data represent means ± SD of nine individual plants.

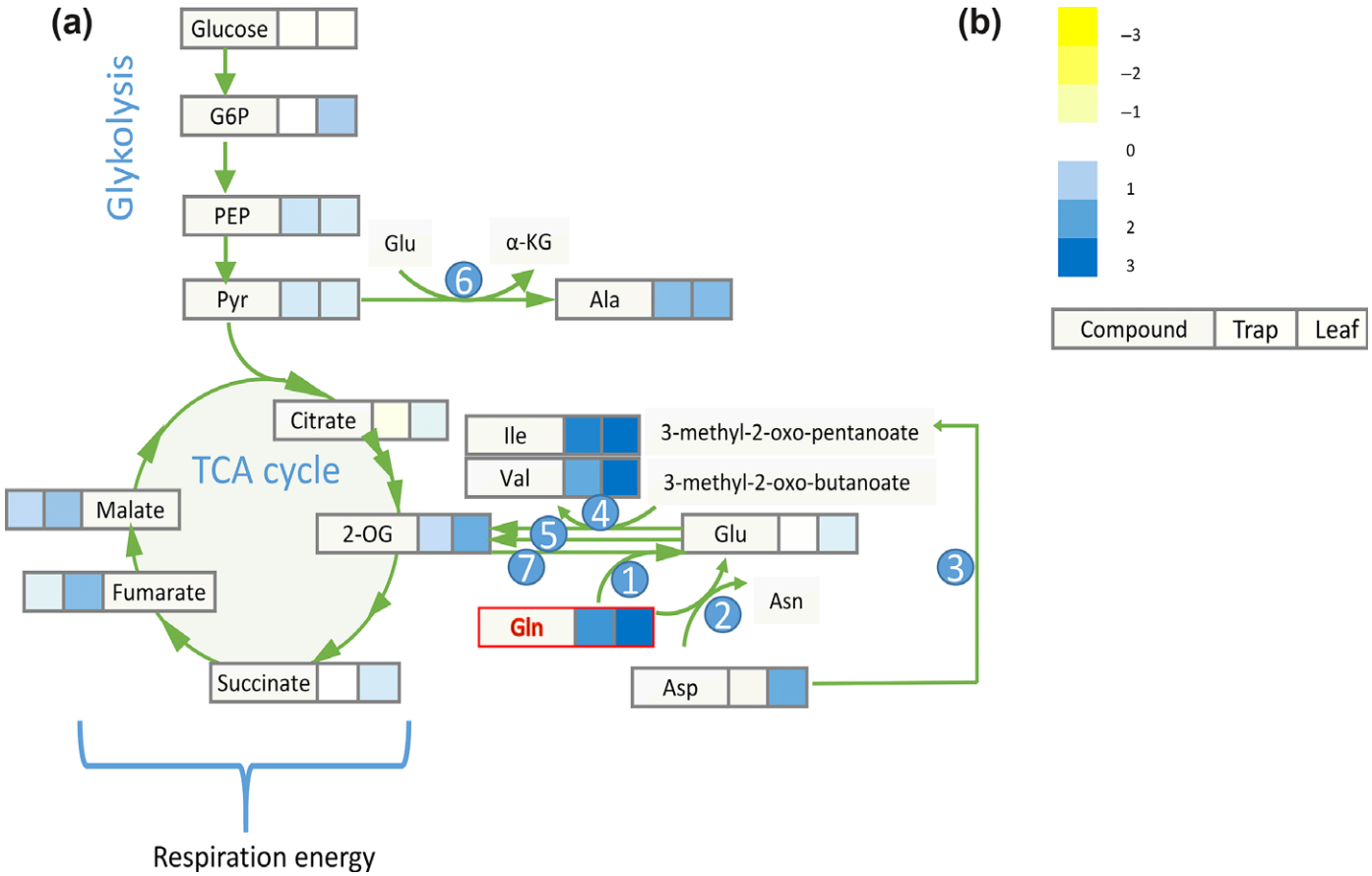

Fig. 3 Influence of Gln feeding to the traps of *Dionaea* plants on the abundance of metabolites of glycolysis and the TCA cycle as well as amino compounds related to these pathways. Compound abundance in traps and leaves of nonfed controls and Gln-fed plants was determined by GC-MS and fold-changes (FC) were calculated. Figure shows $\log_2$ values of fold changes of fed vs nonfed plants at the given color scale (b). Right squares: traps, left squares: leaf blade attached to the trap. Fed Gln is highlighted in red. Numbers in circles represent enzymes catalyzing the pathways involved in amino acid metabolism: (1) L-Gln amino hydrolase; (2) asparagine synthetase; (3) enzymes of the aspartate-derived amino acid pathway (including isoleucine biosynthesis: aspartate kinase, threonine synthase, homoserine dehydrogenase, threonine deaminase); (4) branched-chain aminotransferase forming isoleucine and valine from 3-methyl-2-oxo-pentanoate and 3-methyl-2-oxo-butanoate, respectively; (5) Glu dehydrogenase; (6) alanine aminotransferase; (7) Glu synthase. The Glu decarboxylase pathway (GABA shunt) is not shown because no experimental evidence for this pathway (e.g. GABA abundance) was found in the present study.

Transcription analyses by qRT-PCR revealed minor changes in the abundance of transcripts involved in respiratory Glu degradation and asparagine (Asn) synthesis upon Gln feeding of traps, but these changes were not statistically significant (Fig. S2). Apparently, constitutive transcription of genes mediating respiratory Glu degradation and Asn synthesis are sufficient to channel the C skeleton of Gln derived from prey capture into respiratory energy production. Since changes in metabolic activity can also be achieved by changes in translation, fed traps of *Dionaea* were subjected to proteomic analyses. In these analyses, a total of 450 proteins were identified in traps (Table S2). The increased abundance of ribosomal proteins and elongation factors as well as calreticulin that is involved in protein folding can be interpreted as stimulation of *de novo* protein synthesis in traps fed Gln (Fig. 4). The enhanced protein abundance of pyruvate dehydrogenase in fed traps indicates increased metabolic channeling of C_3 intermediates into the TCA cycle. Enhanced protein abundance of F1F0-ATPase and a NADH oxidoreductase subunit suggest increased activity of the respiratory electron transport chain in response to Gln feeding in traps (Fig. 4). As expected, abundance of Gln synthetase protein declined upon Gln feeding. However, the enzymes involved in respiratory Glu degradation and Asn synthesis were not detected by the proteomic analyses applied.

Discussion

The present labeling experiments with $^{13}C/^{15}N$-Gln show that carnivorous *D. muscipula* can use protein of prey, after depolymerization to amino acids in its external stomach, not only as a source of C and N for growth and development, but also as an alternative respiratory substrate (hypotheses 1 and 2 supported). This is indicated in the present study by $^{13}CO_2$ emission, increased levels of intermediate metabolites of this process, and elevated abundance of proteins of respiratory processes upon $^{13}C/^{15}N$-Gln feeding of traps. The use of prey-derived amino acids as an alternative respiratory substrate by the Venus flytrap is reminiscent of protein degradation in noncarnivorous plants under conditions of high demand for energy, when carbohydrates

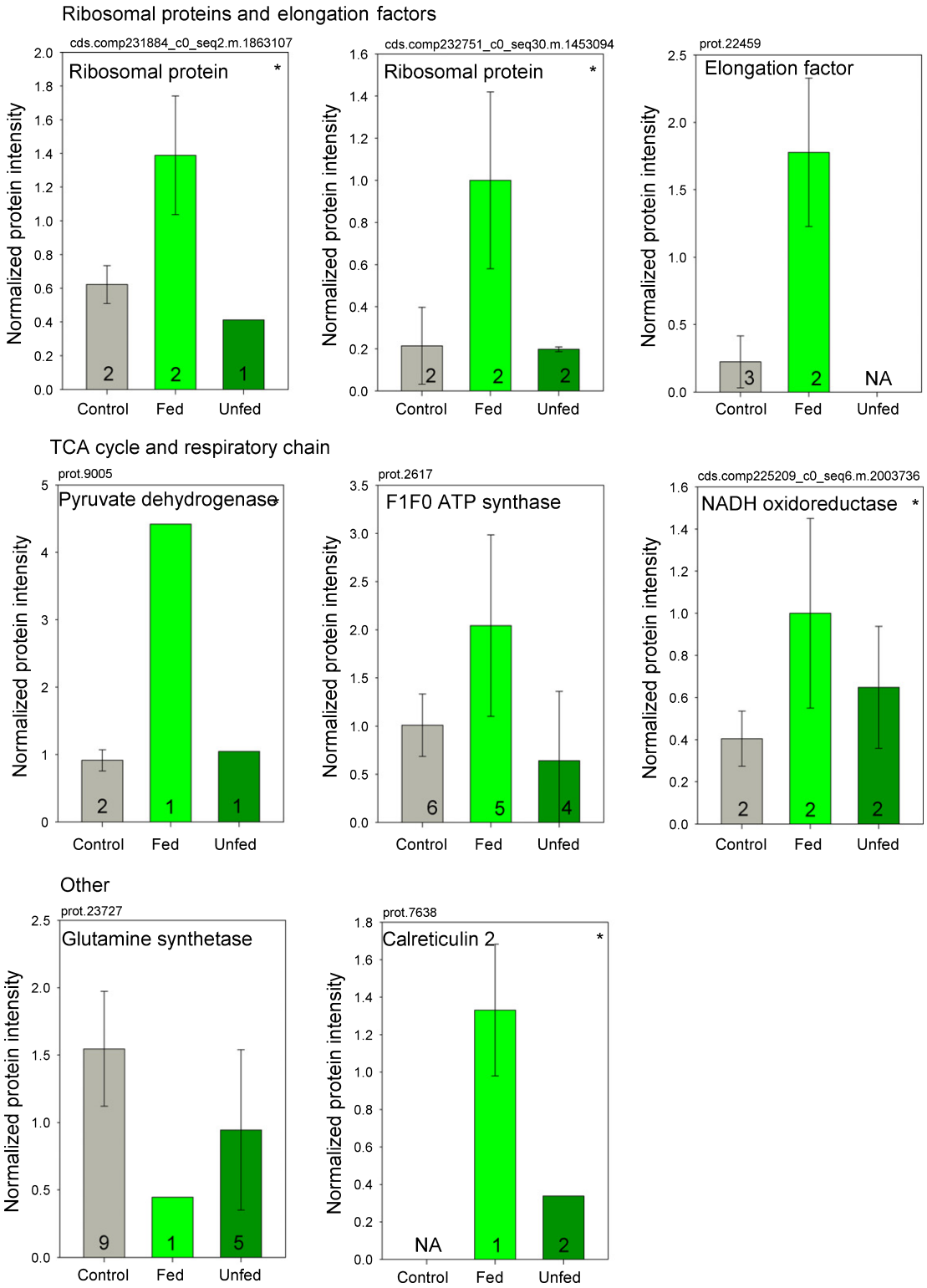

Fig. 4 Normalized protein abundances of selected proteins in fed (light green), unfed (dark green) and control (gray) *Dionaea* traps. Mean values of three biological replicates are shown ± SD. Asterisks indicate significant ($P < 0.05$) differences after one-way ANOVA. Numbers within the bars indicate the numbers of unique peptides identified. Top row, proteins involved in protein synthesis; middle row, proteins involved in respiration; bottom row, other proteins. NA, not available.

are scarce (Araujo *et al.*, 2011). This is frequently observed under stress, but also during germination and senescence (Watanabe *et al.*, 2013; Galili *et al.*, 2014), despite reduced efficiency of respiratory protein catabolism compared to respiration of carbohydrate. This reduced efficiency is indicated by the respiratory quotients of 0.8–0.9 for protein compared to 1.0 for

carbohydrate (Plaxton & Podesta, 2006). However, in *D. muscipula* the use of amino-acid-derived C for respiration is transient and most significant during the initial 25 h of secretion of the prey-decomposing fluid, since $^{13}CO_2$ emission had already started to decline during the 46 h of Gln feeding, even though the respiratory substrate from prey in the glands was not limiting. This view is consistent with previous studies showing that rates of respiration of *D. muscipula* were increased upon prey capture, but only during the initial period of digestion (Pavlovic *et al.*, 2010; Kruse *et al.*, 2014). Apparently, the high energy demand of production and secretion of the prey-decomposing fluid cannot be met by *D. muscipula*'s own resources. The present experiments show that prey-induced enhanced respiration is achieved in *D. muscipula* by both channeling amino-acid-derived C from prey into the TCA cycle and by elevating the abundance of proteins of respiratory electron transport.

The present metabolome data provide evidence for the pathways responsible for channeling Gln-C into the TCA cycle. As expected, Gln feeding caused elevated levels of this amino acid in fed traps and leaves attached to these traps (Fig. 3). Part of the Gln fed was apparently taken up without previous degradation in the prey-decomposing fluid. Surprisingly, the level of Glu, the initial degradation product of Gln, as well as Glu degradation products such as succinate, were not enhanced in traps fed Gln. However, also Gln feeding of tobacco leaf discs did not enhance Glu (Masclaux-Daubresse *et al.*, 2005; Forde & Lea, 2007), but rather 2-oxoglutarate abundance (Schneidereit *et al.*, 2006). These findings fit very well with the present results (Fig. 3), indicating that (1) Gln feeding accelerates Glu turnover at a similar extent as Glu formation from Gln and (2) Gln was initially deaminated to Glu and, subsequently, further degraded to the TCA cycle intermediate 2-oxoglutarate. This second step of Gln degradation can by catalyzed by Glu dehydrogenase and/or several aminotransferases (Figs 3, S1). The involvement of aminotransferase activity in Gln degradation is indicated in the present study by enhanced abundances of Ala as well as Ile and Val in Gln-fed traps. Ala may be produced from Glu by alanine aminotransferase activity, and Ile and Val by Gln-stimulated branched-chain amino acid synthesis (Joshi *et al.*, 2010; Galili *et al.*, 2016). In addition, Ile biosynthesis is linked via Asp to the synthesis of threonine (Thr) that can act as a precursor of Ile (Jander & Joshi, 2009). The two-fold enhanced Thr level in Gln-fed traps of *Dionaea* supports the view of a contribution of this pathway to the elevated Ile level (Table S1). Since Ile and Val can be degraded to succinyl coenzyme A (CoA) and acetyl CoA, which are precursors of TCA cycle intermediates and can directly be used as electron donors of mitochondrial respiration (reviewed by Galili *et al.*, 2016), the enhanced formation of these amino acids in Gln-fed traps are supposed to be linked to respiratory energy formation. It may also be assumed that Glu decarboxylase contributes to Glu degradation in Gln-fed traps of *Dionaea* (Fig. S1). However, we did not find any hints that the GABA shunt is stimulated in response to Gln feeding (Table S1).

Gln feeding of traps did not result in enhanced transcription of enzymes involved in respiratory Gln degradation (Figs S1, S2). Apparently, constitutive expression of these enzymes is sufficient to channel prey-derived Gln-C into respiratory degradation via the TCA cycle. This result is surprising, because amino acid catabolism in noncarnivorous plants is under transcriptional control (Hildebrandt *et al.*, 2015). Whether respiratory Gln degradation in *Dionaea* traps requires enhanced protein abundance or is under biochemical control by metabolic effectors, feedback regulation and post-translational modification, as shown for leaf respiration of noncarnivorous plants (Tcherkez *et al.*, 2012), remains to be elucidated. In the present study, the abundance of the enzymes involved in respiratory Gln degradation could not be detected among the 450 proteins found in traps by the proteomic analysis applied. This is possibly due to the high content of secondary metabolites, which may have suppressed the detection of a significant number of peptides. In this context, it is interesting that a number of ribosomal proteins were increased in abundance in fed traps compared to unfed traps and traps of control plants. A higher content of ribosomal proteins can be associated with higher activity in protein synthesis and growth. In *Arabidopsis*, the occupancy of ribosomes in polysomes underlies diurnal dynamics with high content of polysomes during photosynthetic carbon assimilation in the light (Piques *et al.*, 2009). Similarly, fed traps could have increased resources for protein synthesis and, therefore, afford the investment into higher ribosome protein content, in order to facilitate degradation of prey and the acquisition of prey-derived resources. These results are well in line with recent studies on transcriptome adjustments in active *Dionaea* traps (Bemm *et al.*, 2016). While the pronounced expansion of rough endoplasmatic reticulum in the outer layer of the secretory gland complexes already points to highly active protein synthesis and translocation, insect-fed traps were also considerably enriched in transcripts of ribosomal protein synthesis (Bemm *et al.*, 2016).

The total amount of label acquisition from $^{13}C/^{15}N$-Gln by the traps differed between C and N. From this it is concluded that at least part of the N in the Gln fed is already separated from its C skeleton in the decomposing fluid secreted by the gland cells of the traps (hypothesis 1 supported). Further separation of Gln-N and Gln-C will take place during respiratory decomposition. This conclusion is supported by different allocation of Gln-N and Gln-C into nonfed organs of trap-fed plants. Among these organs, nonfed traps were a stronger sink for Gln-derived C compared to N, supporting the view of poor photosynthetic CO_2 fixation capacity of trap tissue (e.g. Kruse *et al.*, 2014). By contrast, roots were a stronger sink for Gln-derived N compared to C, confirming low N acquisition by *D. muscipula* roots due to low nutrient availability in the soil substrate (Gao *et al.*, 2015). Thus, resources of prey caught by individual traps are distributed within the entire plant, depending on the particular needs of each organ.

The marked increase in respiratory $^{13}CO_2$ release from labeled traps resulted in a clear increase in the $^{13}CO_2$ concentration in the cuvettes (Fig. 2a), which may have been taken up via photosynthetic CO_2 fixation. To estimate the effect of potential ^{13}C labeling via photosynthetic uptake of the green leaf tissue, we calculated the maximum potential uptake of $^{13}CO_2$ taking into account the hours of exposure, the current isotopic composition

in the chambers, as well as the measured photosynthetic CO_2 uptake and isotope discrimination rate of each plant. These calculations suggested that *c.* $2.1 \pm 0.7\%$ of the observed ^{13}C may be attributed to photosynthetic refixation. Thus, all additional ^{13}C observed in nonfed tissue of trap-fed plants can only be explained by long-distance transport in phloem and xylem. We propose that the N-rich amino acid Asn, a well-known N-transport form in plants (Fischer *et al.*, 1998; Finnemann & Schjoerring, 1999; Harrison *et al.*, 2000), might fulfill this function (see Fig. S1). Apparently, fed traps support growth and development of nonfed traps in a similar way by long-distance transport in phloem and xylem, as mature leaves can support young developing leaves in noncarnivorous plants (Herschbach *et al.*, 2012).

The present study provides information on the fate of prey-derived Gln-C and Gln-N in different organs of the Venus flytrap under close to steady state conditions, when traps are still in the process of consuming the Gln fed (Figs 1, 2). With the labeling approach applied, the dynamics of the transition of trap metabolism from the beginning of prey exposure to steady state conditions of prey consumption cannot be characterized. During this transition, metabolic changes may be transient and may follow different time courses. To identify these metabolic changes in response to prey exposure, short time pulse labeling at different times of prey exposure and compound-specific stable isotope analyses by GC- and LC-isotope ratio MS (IRMS) appears to be a useful approach, particularly for the quantification of metabolite fluxes. Obviously, this is a study of its own that will be subject of future research.

Acknowledgements

We thank Cornelia Blessing and Carolin Thöm Chair of Tree Physiology, University of Freiburg, for expert technical assistance during IRMS analyses. We extend our sincere appreciation to the Deanship of Scientific Research at King Saud University for funding this Profilic Research Group (PRG-1436-24).

Author contributions

L.F. planned and performed the labeling experiment, and carried out the $^{13}CO_2$ analyses including data handling; D.M. performed the IRMS and metabolome analyses; J.K. contributed to the labeling experiment, analyzed and evaluated the IRMS and metabolome data, and contributed to the writing of the manuscript; I.K. and D.B. performed the transcriptome analyses including data handling and evaluation, and contributed to the writing of the manuscript; W.X.S. performed the proteome analyses including data handling and evaluation, and contributed to the writing of the manuscript; J.K. contributed to the labeling experiment; S.A. and R.H. contributed to the planning of the experiment and the writing of the manuscript; C.W. contributed to the evaluation of the labeling experiment including the $^{13}CO_2$ analyses and the writing of the manuscript; H.R. had the research idea, contributed to the planning of the experiments and wrote most of the manuscript.

References

Araujo WL, Tohge T, Ishizaki K, Leaver CJ, Fernie AR. 2011. Protein degradation – an alternative respiratory substrate for stressed plants. *Trends in Plant Science* **16**: 489–498.

Bemm F, Becker D, Larisch C, Kreuzer I, Escalante-Perez M, Schulze WX, Ankenbrand M, Van de Weyer AL, Krol E, Al-Rasheid KA *et al.* 2016. Venus flytrap carnivorous lifestyle builds on herbivore defense strategies. *Genome Research* **26**: 812–825.

Böhm J, Krol E, Scherzer S, Kreuzer I, Shabala L, von Meyer K, Shabala S, Al-Rasheid KAS, Rennenberg H, Müller TD *et al.* 2016a. The Venus flytrap *Dionaea muscipula* counts prey-induced action potentials to induce sodium uptake. *Current Biology* **26**: 286–295.

Böhm J, Scherzer S, Shabala S, Krol E, Neher E, Mueller TD, Hedrich R. 2016b. Venus flytrap HKT1-type channel provides for prey sodium uptake into carnivorous plant without conflicting with electrical excitability. *Molecular Plant* **9**: 428–436.

Brewer JS, Baker DJ, Nero AS, Patterson AL, Roberts RS, Turner LM. 2011. Carnivory in plants as a beneficial trait in wetlands. *Aquatic Botany* **94**: 62–70.

Cox J, Mann M. 2008. MaxQuant enables high peptide identification rates, individualized p.p.b.-range mass accuracies and proteome-wide protein quantification. *Nature Biotechnology* **26**: 1367–1372.

Cox J, Neuhauser N, Michalski A, Scheltema RA, Olsen JV, Mann M. 2011. Andromeda: a peptide search engine integrated into the MaxQuant environment. *Journal of Proteome Research* **10**: 1794–1805.

Escalante-Pérez M, Krol E, Stange A, Geiger D, Al-Rasheid KAS, Hause B, Neher E, Hedrich R. 2011. A special pair of phytohormones controls excitabillity, slow closure, and external stomach formation in the Venus flytrap. *Proceedings of the National Academy of Sciences, USA* **108**: 15492–15497.

Farquhar GD, Ehleringer JR, Hubick KT. 1989. Carbon isotope discrimination and photosynthesis. *Annual Review of Plant Physiology and Plant Molecular Biology* **40**: 503–537.

Finke MD. 2013. Complete nutrient content of four species of feeder insects. *Zoo Biology* **32**: 27–36.

Finnemann J, Schjoerring JK. 1999. Translocation of NH_4^+ in oilseed rape plants in relation to glutamine synthetase isogene expression and activity. *Physiologia Plantarum* **105**: 469–477.

Fischer W-F, André B, Rentsch D, Krolkiewicz S, Tegeder M, Breitkreuz K, Frommer WB. 1998. Amino acid transport in plants. *Trends in Plant Sciences* **3**: 188–195.

Forde BG, Lea PJ. 2007. Glutamate in plants: metabolism, regulation, and signaling. *Journal of Experimental Botany* **58**: 2339–2358.

Galili G, Amir R, Fernie AR. 2016. The regulation of essential amino acid synthesis and accumulation in plants. *Annual Review of Plant Biology* **67**: 153–178.

Galili A, Avin-Wittenberg T, Angelovici R, Fernie AR. 2014. The role of photosynthesis and amino acid metabolism in the energy status during seed development. *Frontiers in Plant Science* **5**: 447.

Gao P, Loeffler TS, Honsel A, Krol E, Scherzer S, Kreutzer I, Bemm F, Hedrich R, Rennenberg H, Kruse J. 2015. Integration of trap- and root-derived nitrogen nutrition of carnivorous *Dionaea muscipula*. *New Phytologist* **205**: 1320–1329.

Harrison J, Brugiere N, Phillipson B, Ferrario-Mery S, Becker T, Limami A, Hirel B. 2000. Manipulating the pathway of ammonia assimilation through genetic engineering and breeding: consequences to plant physiology and plant development. *Plant and Soil* **221**: 81–93.

Herschbach C, Gessler A, Rennenberg H. 2012. Long-distance transport and plant internal cycling of N- and S-compounds. *Progress in Botany* **73**: 161–188.

Hildebrandt TM, Nesi AN, Araujo WL, Braun H-P. 2015. Amino acid catabolism in plants. *Molecular Plant* **8**: 1563–1579.

Ichiisi S, Nagamitsu T, Kondo Y, Iwashina T, Kondo K, Tagashira N. 1999. Effects of macro-components and sucrose in the medium on *in vitro* red-color pigmentation in *Dionaea muscipula* Ellis and *Drosera spathulata* Labill. *Plant Biotechnology* **16**: 235–238.

Jaffe MJ. 1973. Role of ATP in mechanically stimulated rapid closure of Venus-flytrap. *Plant Physiology* **51**: 17–18.

Jander G, Joshi V. 2009. Aspartate-derived amino acid biosynthesis in *Arabidopsis thaliana*. *Arabidopsis Book* **7**: e0121.

Joel DM, Juniper BE, Dafni A. 1985. Ultraviolet patterns in the traps of carnivorous plants. *New Phytologist* **101**: 585–593.

Joshi V, Joung JG, Fei Z, Jander G. 2010. Interdependence of threonine, methionine and isoleucine metabolism in plants: accumulation and transcriptional regulation under abiotic stress. *Amino Acids* **39**: 933–947.

Kopka J, Schauer N, Krueger S, Birkemeyer C, Usadel B, Bergmuller E, Dormann P, Weckwerth W, Gibon Y, Stitt M *et al.* 2005. GMD@CSB.DB: the Golm Metabolome Database. *Bioinformatics* **21**: 1635–1638.

Kreuzwieser J, Hauberg J, Howell KA, Carroll A, Rennenberg H, Millar AH, Whelan J. 2009. Differential response of gray poplar leaves and roots underpins stress adaptation during hypoxia. *Plant Physiology* **149**: 461–473.

Kreuzwieser J, Scheerer U, Honsel A, Kruse J, Burzlaff T, Alfarraj S, Georgiev P, Schnitzler J-P, Ghirardi A, Kreuzer I *et al.* 2014. Venus fly trap attracts insects by the release of volatile organic compounds. *Journal of Experimental Botany* **65**: 755–766.

Kruse J, Gao P, Honsel A, Kreuzwieser J, Burzlaff T, Alfarraj S, Hedrich R, Rennenberg H. 2014. Strategy of nitrogen acquisition and utilization by carnivorous *Dionaea muscipula*. *Oecologia* **174**: 839–851.

Kurup R, Johnson AJ, Sankar S, Hussain AA, Kumar CS, Sabulal B. 2013. Fluorescent prey traps in carnivorous plants. *Plant Biology* **15**: 611–615.

Libiakova M, Flokova K, Novak O, Slovakova L, Pavlovic A. 2014. Abundance of cysteine endopeptidase dionain in digestive fluid of Venus flytrap (*Dionaea muscipula* Ellis) is regulated by different stimuli from prey through jasmonates. *PLoS ONE* **9**: e104424.

Mariod AA, Abdel-Wahab SI, Ain NM. 2011. Proximate amino acid, fatty acid and mineral composition of two Sudanese edible pentatomid insects. *International Journal of Tropical Insect Science* **31**: 145–153.

Masclaux-Daubresse C, Carrayol E, Valadier M-H. 2005. The two nitrogen mobilisation- and senescence-associated GS1 and GDH genes are controlled by C and N metabolites. *Planta* **221**: 580–588.

Paszota P, Escalante-Perez M, Thomsen LR, Risor MW, Demski A, Sanglas L, Lielsen TA, Karrig H, Thogersen IB, Hedrich R *et al.* 2014. Secreted major Venus flytrap chitinase enables digestion of arthropod prey. *Biochimica et Biophysica Acta* **1844**: 374–383.

Pavlovic A, Demko V, Hudak J. 2010. Trap closure and prey retention in Venus flytrap (*Dionaea muscipula*) temporarily reduces photosynthesis and stimulates respiration. *Annals of Botany* **105**: 37–44.

Pavlovic A, Slovakova L, Pandolfi C, Mancuso S. 2011. On the mechanism underlying photosynthetic limitation upon trigger hair irritation in the carnivorous plant Venus flytrap (*Dionaea muscipula* Ellis). *Journal of Experimental Botany* **62**: 1991–2000.

Piques MC, Schulze WX, Höhne M, Usadel B, Gibon Y, Rohwer J, Stitt M. 2009. Ribosome and transcript copy numbers, polysome occupancy and enzyme dynamics in *Arabidopsis*. *Molecular Systems Biology* **5**: E1–E17.

Plaxton WC, Podesta FE. 2006. The functional organization and control of plant respiration. *Critical Reviews in Plant Sciences* **25**: 159–198.

Priault P, Wegener F, Werner C. 2009. Pronounced differences in diurnal variation of carbon isotope composition of leaf respired CO_2 among functional groups. *New Phytologist* **181**: 400–412.

Rennenberg H, Herschbach C. 2014. A detailed view on sulphur metabolism at the cellular and whole plant level illustrates challenges in metabolite flux analyses. *Journal of Experimental Botany* **65**: 5711–5724.

Roberts PR, Oosting HJ. 1958. Resonses of Venus fly trap (*Dionaea muscipula*) to factors involved in its endemism. *Ecological Monographs* **28**: 193–217.

Schaefer HM, Ruxton GD. 2008. Fatal attraction: carnivorous plants roll out the red carpet to lure insects. *Biology Letters* **4**: 153–155.

Scherzer S, Böhm J, Krol E, Shabala L, Kreuzer I, Larisch C, Bemm F, Al-Rasheid KAS, Shabala S, Rennnenberg H *et al.* 2015. Calcium sensor kinase activates potassium uptake in gland cells of Venus flytraps. *Proceedings of the National Academy of Sciences, USA* **112**: 7309–7314.

Scherzer S, Krol E, Kreuzer I, Kruse J, Escalante-Perez M, Karl F, Müller T, Rennenberg H, Al-Rascheid KAS, Neher E *et al.* 2013. The *Dionaea muscipula* ammonium channel DmAMT1 provides NH_4^+ uptake associated with Venus flytrap's prey digestion. *Current Biology* **23**: 1649–1657.

Schneidereit J, Häusler RE, Fien G, Kaiser W, Weber W, Weber APM. 2006. Antisense repression reveals a crucial role of the plastidic 2-oxoglutarate/malate translocator DiT1 at the interface between carbon and nitrogen metabolism. *Plant Journal* **45**: 206–224.

Schulze WX, Sanggaard KW, Kreuzer I, Knudsen AD, Bemm F, Thogersen IB, Brautigam A, Thomsen LR, Schliesky S, Dyrlund TF *et al.* 2012. The protein composition of the digestive fluid from the Venus flytrap sheds light on prey digestion mechanisms. *Molecular and Cellular Proteomics* **11**: 1306–1319.

Tcherkez G, Bligny R, Gout E, Mahé A, Hodges M, Cornic G. 2008. Respiratory metabolism of illuminated leaves depends on CO_2 and O_2 conditions. *Proceedings of the National Academy of Sciences, USA* **105**: 797–802.

Tcherkez G, Boex-Fontvieille E, Mahé A, Hodges M. 2012. Respiratory carbon fluxes in leaves. *Current Opinion in Plant Biology* **15**: 308–314.

Watanabe M, Balazadeh S, Tohge T, Erban A, Giavalisco P, Kopka J, Mueller-Roeber B, Fernie AR, Hoefgen R. 2013. Comprehensive dissection of spaciotemporal metabolic shifts in primary, secondary and lipid metabolism during developmental senescence in *Arabidopsis*. *Plant Physiology* **162**: 1290–1310.

Williams SE, Bennett AB. 1980. Leaf closure in the Venus flytrap – an acid growth-response. *Science* **218**: 1120–1122.

Wu XN, Schulze WX. 2015. Phosphopeptide profiling of receptor kinase mutants. *Methods in Molecular Biology* **1306**: 71–79.

Zauber H, Schulze WX. 2012. Proteomics wants cRacker: automated standardized data analysis of LC/MS derived proteomic data. *Journal of Proteome Research* **11**: 5548–5555.

Supporting Information

Additional Supporting Information may be found online in the Supporting Information tab for this article:

Fig. S1 Literature-based model of respiratory Gln degradation.

Fig. S2 Transcription of selected *Dionaea* genes involved in respiratory Gln degradation.

Table S1 Metabolome analyses of *Dionaea* tissues

Table S2 Proteome analyses of *Dionaea* tissues

Please note: Wiley Blackwell are not responsible for the content or functionality of any Supporting Information supplied by the authors. Any queries (other than missing material) should be directed to the *New Phytologist* Central Office.